Ultra Low Energy (ULE) Implant Dose And Activation Monitoring

Robert Hillard[1], John Borland[2], and Mark Benjamin[1],

[1]Solid State Measurements, Inc., 110 Technology Dr., Pittsburgh, PA 15275
[2]J.O.B. Technologies, 5 Farrington Lane, South Hamilton, MA 01982
e-mail: rhillard@ssm-inc.com

1. Introduction

MOS device performance is heavily related to the design of Source-Drain Ultra-shallow junctions. Source-Drain Extensions (SDE) process and design technology are critical in existing and future device development. Critical device parameters such as on-state drive current ($I_{DS, ON}$) are highly dependent on the SDE series resistance (R_{DS}). It is therefore desirable to have SDE structures that have low sheet resistances. This requires SDE structures with high carrier densities. At the same time, Threshold Voltage (V_T) roll-off due to Short Channel Effects (SCE) increases as the channel length is decreased [1,2,3]. These effects need to be minimized. This requires producing a "rectangular" overall device structure [4] where the gate dielectric thickness, SDE junction depths and channel carrier profile are thin. Highly abrupt, steep gradient carrier density profiles are also necessary in order to reduce SCE via channel charge sharing [3]. Careful consideration of all of these device performance issues leads to the fact that the SDE carrier density profiles must be highly abrupt "Box" type profiles with a high peak carrier density and a shallow junction depth (x_j). As an example, SDE structures with activated dopant densites at or near solid solubility with x_j's less than 20 nm are under development for the 65 nm technology node.

Ultra-Shallow Junction (USJ) structures require careful process design of the Pre-amorphization implant, SDE implant and the dopant activation and implant anneal. The USJ junction depths and level of dopant activation depend strongly on processing [5]. The best method for monitoring the USJ structure is with Four Point Probe (4pp) Sheet Resistance (R_S) measurements[6,7,8]. The measured R_S is highly sensitive to the activated carrier density and x_j. This is a highly accurate, absolute method that has been used successfully on structures with deeper junction depths and layer thicknesses. Conventional 4pp R_S measurements generally use four penetrating, scrubbing probes placed in contact with the top layer of the semiconductor wafer. It is necessary for conventional 4pp probes to penetrate through any existing native oxide that exists on the semiconductor surface in order to make good electrical contact to the top semiconductor layer. A common problem that now exists in the industry is the conventional 4pp method penetrates through USJ SDE structure into the semiconductor substrate. Under these circumstances, the R_S of the underlying substrate is measured. Generally this results in low R_S values and all sensitivity to the top USJ layer is lost.

The sheet resistance alone is not enough to qualify the USJ layer. Sheet resistance is sensitive to both activation level and junction depth. In order to differentiate these two parameters, it is desirable to have quality methods that can measure both of these. The junction depth can be measured with Secondary Ion Mass Spectrosopy (SIMS) [6,8] or, in some cases, Ultra-shallow Layer(USL) Spreading Resistance Profiling (SRP) [4,8]. Determination of the Electrically Active Surface Dopant Density(N_{SURF}) is the primary parameter of interest for monitoring dopant activation. Up to now there have been no known methods for measuring N_{SURF} directly. It can be estimated from slope changes in SIMS profiles but since SIMS measures atomic density, there is always some uncertainty.

This paper describes newly developed techniques to accurately measure the 4pp sheet resistance without the influences of probe penetration. Also, the Electrically Active Surface Dopant Density (N_{SURF}) is measured directly with a single non-penetrating, non-damaging and non-contaminating EM-Probe[9,10,11]. The technique is Capacitance-Voltage(CV) based[11,12,13] and measures the average N_{SURF} within about 1 nm. from the top surface of a USJ structure.

These new technologies offer measurements with probes that are non-penetrating, non-damaging and non-contaminating. Both of the methods described can be used on blanket wafers and the N_{SURF} measurement can be made in scribe line test areas with a minimum geometry as small as 80 μm[11].

2. EM-Probe Description

A basic description of an EM-Probe Metal-Oxide Semiconductor Capacitor (MOSCAP) structure is shown in Figure 1.

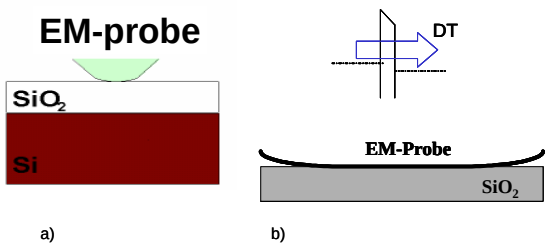

Figure 1: Schematics of an EM-Probe MOSCAP.

The EM-Probe MOSCAP shown in Figure 1 is formed by using a specially prepared probe [9, 10, 11].

Generally, a metal is used. There are two types of EM-Probes available; one for Capacitance-Voltage (CV) applications and the other for Current-Voltage (IV) applications. These are generally referred to as Type A and Type C probes respectively. Type A CV probes have an inherent metal oxide present on the probe surface. This oxide serves as a barrier to current flow and allows for CV measurements on thin dielectrics without the effects of leakage current [11]. Type C probes are made of a metal whose properties are such that no or little metallic oxide forms on the probe and, the oxide that does form is conductive. These properties make the Type C probe ideal for IV applications. All EM-Probes are mounted on a kinematic bearing system with controlled descent and ascent. The kinematic system ensures that no probe scrubbing occurs.

The EM-Probe contacts shown in Figure 1 are formed by lowering the probe onto a semiconductor surface or dielectric and elastically deforming the probe material. The resultant contact diameter is typically 40 to 60 um and depends on the probe geometry and applied force. EM-Probe MOSCAPs formed in the manner discussed have been used to measure CV and IV on oxides as thin as 0.7 nm [11]. An example of an EM-Probe CV measurement on a thin dielectric is shown in Figure 2. The substrate is p-type.

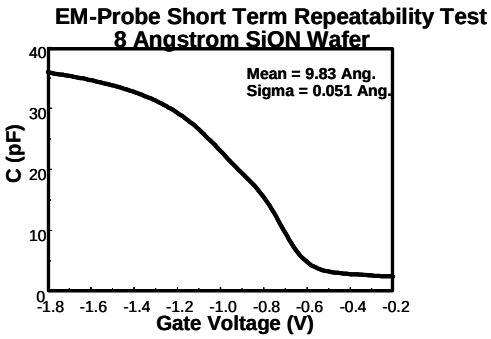

Figure 2: EM-Probe CV curve measured on an 0.8 nm oxide.

Fifteen measurements were made in a local area, raising and lowering the probe prior to each new measurement. The mean CET and one sigma standard deviation was 0.983 nm. and 0.0051 nm. respectively. The CV data shown in Figure 2 are of high quality and verify that leakage current is low and that the EM-Probe is non-penetrating.

A close-up illustration depicting the major mechanical differences between Conventional and EM probes is given in Figure 3. The primary advantage of the EM-Probe is that it is non-penetrating and can be used to measure all foreseeable USJ structures without the effects of probe penetration.

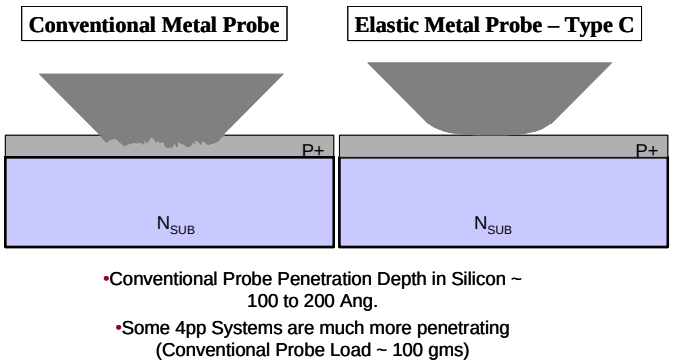

Figure 3: Another illustration pointing out the penetrating versus non-penetrating nature of the Conventional and EM-Probe 4pp designs.

3. EM-Probe 4pp Sheet Resistance Applications Examples

We present an example of EM-Probe 4pp measurements on USJ S/D structures

Seven boron implanted USJ S/D wafers were evaluated with both scrubbing and less penetrating 4pp and the EM-probe 4pp. The junction depths determined from SIMS are between 12 nm. And 30 nm. The typical SIMS atomic profile is shown in Figure 4. Each wafer received a standard 550C/1hour anneal. There is a Ge-PAI process to a depth of 12 nm for each wafer as well.

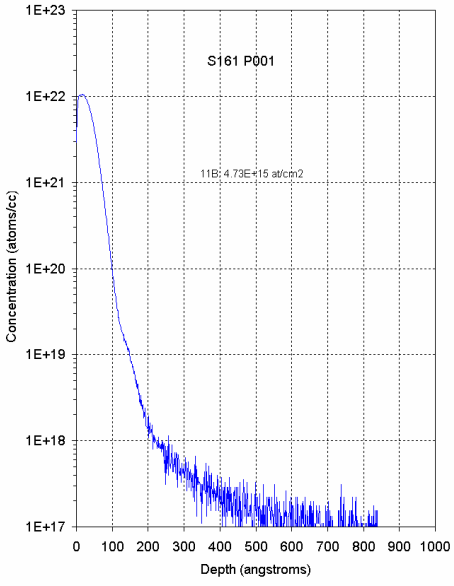

Figure 4: SIMs profile for wafer S161

Scrubbing but less penetrating SR type probes were installed first to do the Rs measurements and the probes were aligned with a horizontal, in-line array at probe spacing of 1.59 mm.

The 4pp system was then setup with four Type C elastic probes to repeat the R_S measurements. These probes were aligned in a vertical, in-line array. The probe spacing was set to about ~2.8 mm. This was determined to be the smallest possible for the new probe/mount design available.

The probe space can be reduced further if the weight of each probe arm is trimmed in a certain angle.

During experiments, the configuration switching method was used for all sheet resistance measurements and each sample was measured using the ASTM-F84 specified 10pt pattern. The results are shown in Figure 5.

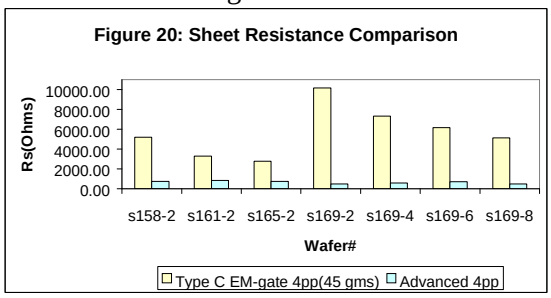

Figure 5: Sheet resistance data measured with both scrubbing and EM-probe 4pp systems.

It is clear that the backside sheet resistance measured by both EM-probe and advanced SR type probes are in close agreement, both data are around 44 ohm per square. However, the front side sheet resistance of each wafer is much different between these two kinds of measurements. Again, the EM-probe measurement gives much higher sheet resistance and indicates the penetrating behavior of the scrubbing less penetrating probes.

For further investigation, three of the seven samples were sent out for non-damaging, non-penetrating Hg-probe 4pp measurements. These data were in excellent agreement with the EM-probe 4pp measurements and in turn verify none penetrating advantage of using EM-probe 4pp. The data are shown in Figure 6.

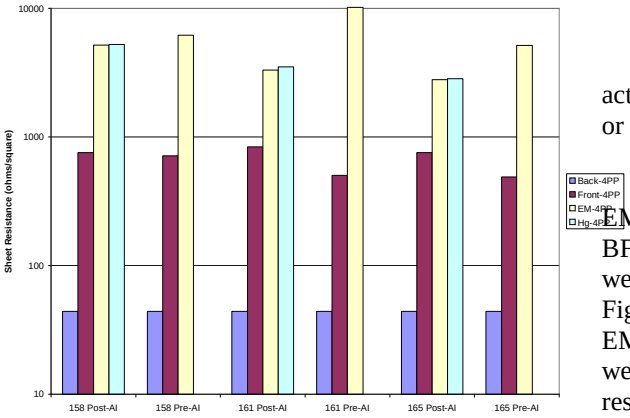

Figure 6: Sheet resistance data measured with advanced 4pp, EM-probe 4pp and Hg 4pp.

Mapping capability is also highly useful. Variations in Dose and sheet resistance reveal valuable information about the ion implantation and annealing processes. An example of an R_S map is shown in Figure 7

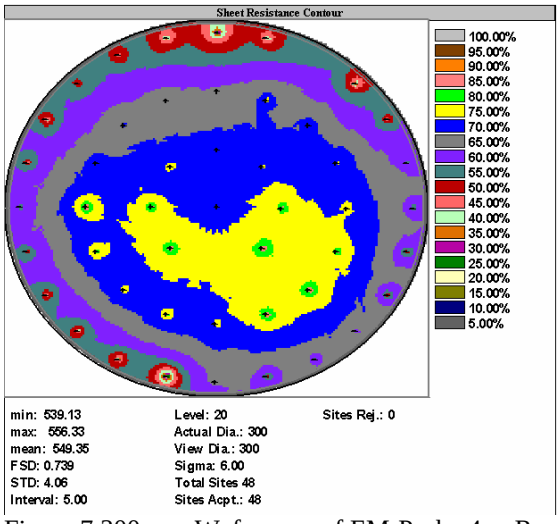

Figure 7 300 mm Wafer map of EM-Probe 4pp R_S.

4. EM-Probe CV Based N_{SURF} Applications Example

Prior to discussing specific examples, it should be clarified that N_{SURF} is highly dependent upon activation level and will correlate with sheet resistance in those cases where activation modifications are made. Poor N_{SURF} correlation with R_S will be expected in cases where the surface activation is constant but the junction depth is changing. These two cases are illustrated in Figure 8.

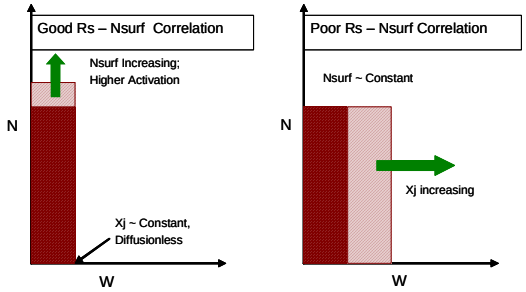

Figure 8 Two profiles showing that either activation level or increased diffusion (deeper junction) or both can be modified.

P+/N USJ Structures(x_j = 15 to 25 nm)

In this case, EM-Probe 4pp sheet resistance and EM-Probe CV measurements were made on a matrix of BF_2 implanted samples. Both activation and diffusion were affected b y the processing for these samples. Figure 9 shows the results of EM-Probe 4pp R_S and EM-Probe CV N_{SURF} measurements. Values of $1/N_{SURF}$ were plotted against R_S consistent with the fact that resistance is inversely proportional to Dopant Density.

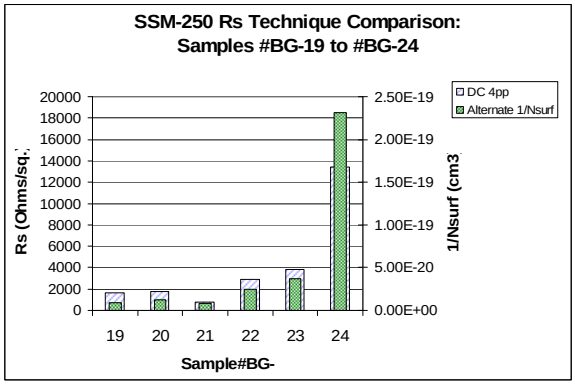

Figure 9 Histogram comparison of EM-Probe 4pp R_S and EM-Probe N_{SURF}.

The measured EM-probe CV curves for the sample results shown in Figure 9 are provided in Figure 10.

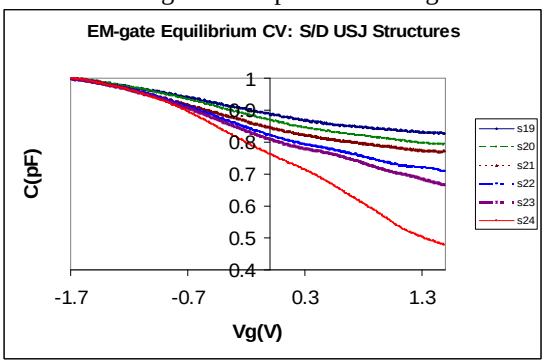

Figure 10 Normalized EM-probe CV curves obtained on the samples shown in Fig. 13. The values of N_{SURF} are obtained from the measured maximum and minimum capacitances.

A correlation plot of EM-Probe 4pp R_S and EM-Probe N_{SURF} for all of the groups measured is shown in Figure 11. Good correlation is observed for this case

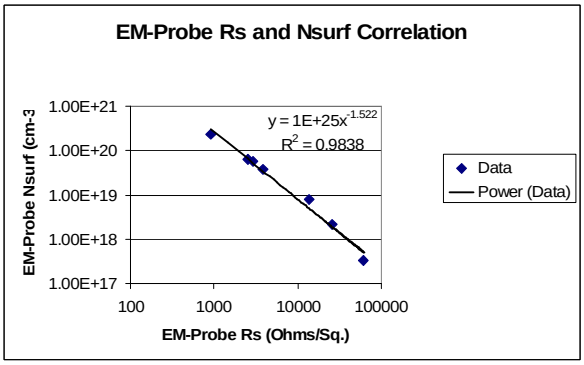

Figure 11 Correlation plot of EM-Probe N_{SURF} versus EM-Probe 4pp R_S.

Summary

EM-probe 4PP R_S measurements were described and it was demonstrated that valid measurements have been made of thin junctions. Several samples were presented. It was found that the EM-probe 4PP could measure SDE structures with junction depths of 15 nm. Conventional 4PP were found to be limited to about 30 to 40 nm and deeper.

We introduce an alternate method of characterizer the surface electrically active dopant and show that it is a powerful characterization tool for diffusionless annealing.

References

[1] 45nm CMOS Technology, IEDM 2004 Short Course, IEEE 2004

[2] S. Wolf, *Silicon Processing for the VLSI Era, Volume 3*,(1995) Chp. 3

[3] Sub-100nm CMOS, IEDM Conference Short Course 1999 (1999)

[4] USJ Conference Short Course, Sixth International Workshop on Fabrication, Characterization, and Modeling of Ultra-Shallow Doping Profiles in Semiconductors, Napa, CA. 2001

[5] R.J. Hillard, R.G. Mazur, W.J. Alexander,, C.W. Ye, ,M.C. Benjamin,and J.O. Borland,. *Silicon Front-End Junction Formation—Physics and Technology*, (2004) C11.6

[6] D.K. Schroder, *Semiconductor Material and Device Characterization*, (1990)

[7] D.S. Perloff, et .al, *Solid State Technology*, February 1981, p. 112.

[8] J.O. Borland, *Solid State Technology*, June 2002

[9] R. Hillard, "Accurate Determination of Ultra-shallow Layer Sheet resistance with a Non-penetrating Four Point Probe", *Semicon-West 2004 Workshop on USJ Characterization* (2004)

[10] M.C. Benjamin, R.J. Hillard, and J.O. Borland., IIT Conference 2004, Taiwan. (in press)

[11] R.J. Hillard, et .al, *Characterization and Metrology for ULSI Technology*, AIP Conference proceedings Vol. 683, (2003) p. 802.

[12] E. Nicollian, J.R. Brews., *MOS Physics and Technology*, (1981) p. 148

[13] S.M. Sze,, *Physics of Semiconductor Devices*,, (1981) ch. 7

[14] R.G. Mazur, *Materials and Process Characterization of Ion Implantation*, (1997) ch. 3.1